Talanta 117 (2013) 152–157

Contents lists available at ScienceDirect

Talanta

journal homepage: www.elsevier.com/locate/talanta

The electron-transfer based interaction between transition metal ions and photoluminescent graphene quantum dots (GQDs): A platform for metal ion sensing

Hongduan Huang [a], Lei Liao [b], Xiao Xu [a], Mingjian Zou [a], Feng Liu [a], Na Li [a,*]

[a] Beijing National Laboratory for Molecular Sciences (BNLMS), Key Laboratory of Bioorganic Chemistry and Molecular Engineering of Ministry of Education, Institute of Analytical Chemistry, College of Chemistry and Molecular Engineering, Peking University, Beijing 100871, PR China
[b] Center for Nanochemistry, Beijing National Laboratory for Molecular Sciences (BNLMS), State Key Laboratory for Structural Chemistry of Unstable and Stable Species, College of Chemistry and Molecular Engineering, Peking University, Beijing 100871, PR China

ARTICLE INFO

Article history:
Received 28 May 2013
Received in revised form
16 August 2013
Accepted 28 August 2013
Available online 4 September 2013

Keywords:
Graphene quantum dots
Transition metal ions
Photoluminescence
Quenching

ABSTRACT

The electron-transfer based quenching effect of commonly encountered transition metal ions on the photoluminescence of grapheme quantum dots (GQDs) was for the first time investigated, and was found to be associated with electron configuration of the individual metal ion. Ethylene diamine tetraacetic acid (EDTA), the metal ion chelator, can competitively interact with metal ions to recover the quenched photoluminescence of GQDs. Basically, metal ions with empty or completely filled *d* orbits could not quench the photoluminescence of GQDs, but this quenching effect was observed for the metal ions with partly filled *d* orbits. Based on the quenching-recovering strategy, a simple optical metal sensing platform was established by taking Ni^{2+} as an example. Using the nickel ion-specific chelating reagent, dimethylglyoxime (DMG), to replace EDTA, a detection limit of 4.1 μM was obtained in standard solution. This proposed strategy does not need further functionalization of GQDs, facilitating the application for simple, fast and cost-effective screening of metal ions.

1. Introduction

Graphene quantum dots (GQDs), a new kind of carbon-based photoluminescent nanomaterial, are emerging as a significant research area in recent years since the discovery by Dai and co-workers in 2008 [1]. GQDs are superior to common carbon dots (CDs) because the nature of nano-sized single-layer graphene oxide sheets endows them with ultrahigh specific surface area [1], making GQDs more sensitive to micro-environmental changes. And the structurally well-defined GQDs are more favorable for structural characterization and theoretical simulation [2–5], comparing with common CDs which usually contain amorphous carbon. So far, much effort has been paid to the biological applications of GQDs, e.g. bioimaging and electrochemical biosensing [6–9], and catalysis [10]. Meanwhile, attractive optoelectronic properties of GQDs owing to the nano-sized dimension, which were distinctive from the graphene sheets, also found significant applications in organic photovoltaics as well as organic light-emitting diodes [11–13]. Although CDs have found some applications [14–21], great effort is necessary to best use excellent structural and optical properties of GQDs in optical sensing applications [22–25].

Metal ions can easily interact with GQDs because of the π-systems as well as carboxyl and hydroxyl groups on the edges and surfaces. Herein, we for the first time carried out a systematic evaluation of the quenching effect of commonly encountered transition metal ions (Sc^{3+}, Cr^{3+}, Mn^{2+}, Fe^{3+}, Co^{2+}, Ni^{2+}, Cu^{2+}, Zn^{2+}, Ru^{3+}, Ag^{+}, Cd^{2+}, and Hg^{2+}) on the photoluminescence (PL) of GQDs, with which GQDs were prepared with an improved method reported elsewhere [26]. With GQDs as both the chelator and fluorophore and ethylene diamine tetraacetic acid (EDTA) as the competitive chelator, quenching-recovering performance of the above metal ions on the photoluminescence of GQDs can be categorized into three groups (Scheme 1): in the non-quenching group, metal ions show no quenching effect; in the quenching-recovering group, metal ions quench the photoluminescence of GQDs and the luminescence can be recovered with addition of EDTA; in the quenching-non-recovering group, metal ions quench the photoluminescence of GQDs but the luminescence cannot be recovered with addition of EDTA.

To demonstrate the proof-of-concept of sensing metal ions using the quenching-recovery strategy, a simple, rapid and selective detection method was developed by taking Ni^{2+} as an example, in which dimethylglyoxime (DMG) was used to replace

* Corresponding author. Tel.: +86 10 62761187; fax: +86 10 62751708.
E-mail address: lina@pku.edu.cn (N. Li).

0039-9140/$ - see front matter © 2013 Elsevier B.V. All rights reserved.
http://dx.doi.org/10.1016/j.talanta.2013.08.055

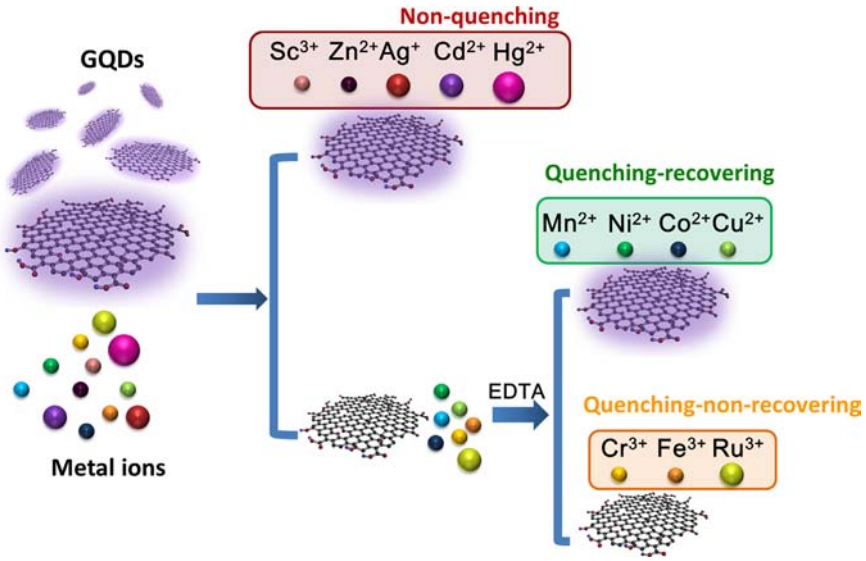

Scheme 1. Schematics showing the group performance of quenching and recovering effect of transition metal ions on the photoluminescence of GQDs.

EDTA as the competitive chelating reagent to specifically react with Ni^{2+}. The quenching-recovering strategy actually is a turn-on detection mode, which assures a low-background signal. This new optical detection method was simple, fast, and versatile, which can be applied to sensing other metal ions in the quenching-recovering group when the specific chelator is used. Furthermore, this study helps with more profound understanding of the interaction mechanism between GQDs and analytes and better extending the application of GQDs in the optical sensing field.

2. Materials and methods

2.1. Materials and apparatus

H_2SO_4 (AR), HNO_3 (AR), HCl (AR), NaOH (AR), Na_2CO_3 (AR), $NH_3 \cdot H_2O$ (AR), dimethylglyoxime (DMG, AR), Ethylene diamine tetraacetic acid (EDTA, AR), $RuCl_3$ (AR), Sc_2O_3 (99%), $AgNO_3$ (AR), $Hg(NO_3)_2$ and $ZnSO_4$ (AR) were purchased from Beijing Chemical Works. Trizma base (AR) was purchased from Beijing Xinjinke Biotechnology Co., Ltd. $CuSO_4$ (AR) and $FeCl_3$ (AR) were purchased from Sinopharm Chemical Reagent Co., Ltd. $MnCl_2$ (AR) was purchased from Shantou Xinlong Factory (Guangdong). $NiCl_2$ (AR), $CoCl_2$ (AR), and $CrCl_3$ (AR) were purchased from Beijing Shuanghuan Chemical Reagent Co., Ltd. $CdSO_4$ (GR) was purchased from Beijing institute of chemical reagents. Wahaha® purified water was used throughout the study.

Metal salts ($MnCl_2$, $CrCl_3$, $FeCl_3$, $NiCl_2$, $CoCl_2$, $CuSO_4$, $ZnSO_4$, $RuCl_3$, $CdSO_4$, $AgNO_3$, and $Hg(NO_3)_2$) were dissolved in specific diluted acid matching the anion of the individual metal salt to yield a final concentration of 100 mM. Specifically, the diluted acid was prepared from concentrated acid at the volumetric ratio of $V(H_2O):V(\text{acid})=299:1$ to prevent hydrolysis of metal ions. Sc_2O_3 was dissolved in 5 M HCl to make a final concentration of 100 mM. To minimize the acid effect on determination, extra HCl was neutralized by 5 M NaOH before using.

Tris-acid buffer stock solutions (Tris–$HCl/HNO_3/H_2SO_4$) were prepared by dissolving trizma base in water to make a concentration of 100 mM. The specific concentrated acid, matching the anion of the individual metal salt, was then added to adjust the pH to 8.5. DMG was dissolved in 14% ammonia solution to obtain a 100 mM stock solution. The working solution was obtained by diluting the stock solution with 14% ammonia solution to the concentration as indicated.

2.2. Preparation of GQDs

GQDs were prepared by chemical oxidation of carbon fibers (Tebao Corporation, Beijing) with an improved method reported elsewhere [26]. Briefly, 0.15 g carbon fiber was immersed in the mixture of concentrated acid (H_2SO_4:HNO_3=10 mL: 30 mL) and sonicated for 2 h, followed by the refluxing at 150 °C for 24 h. After pH adjustment to 8 by Na_2CO_3, the mixture was filtered through a 0.22 μM filter membrane. The final GQD product was obtained by dialyzing the filtered solution in a dialysis bag (2000 Da) for 3 days.

2.3. Characterization of GQDs

Photoluminescence profiles were obtained with the Hitachi F-7000 spectrofluorometer (Hitachi Co. Ltd., Japan). UV–vis absorption spectra were recorded with a Hitachi U-3100 spectrophotometer (Hitachi Co. Ltd., Japan). Fourier transform infrared (FTIR) spectra were obtained with an FTIR spectrophotometer (Thermo Scientific Nicolet iN 10 MX). Transmission electron microscopy (TEM) and high-resolution transmission electron microscopy (HRTEM) measurements were performed with the H-9000 (JEOL Ltd., Japan) and JEM-2100F (JEOL Ltd., Japan) transmission electron microscopes, respectively. Atomic force microscopy (AFM) images were collected using a Vecco IIIa nanoscope using the tapping mode. Raman spectra were measured using a Raman Imaging Microscope System (Horiba, HR 800) with a 633 nm laser. X-ray photoelectron spectroscopy (XPS) was measured with a Kratos Axis Ultra-DLD XPS System (Kratos Analytical Ltd., Japan).

2.4. Photoluminescence response of GQDs against metal ions

A volume of 5 L of GQD stock solution was diluted to 400 L in 10 mM Tris–$HCl/H_2SO_4/HNO_3$ buffer (pH 8.5). A volume of 4 L of metal ions with concentration as indicated was added to the GQD solution. After 5 min at room temperature, photoluminescence of the mixture was measured. A volume of 20 L of 5 mM DMG ammonia solution was added to the GQD–metal ion mixture and centrifuged with 13,000 rpm for 15 min. The supernatant was collected and photoluminescence intensity was measured.

3. Results and discussion

3.1. Preparation and characterization of GQDs

GQDs were prepared by oxidizing and cutting micrometer-sized pitch-based carbon fiber (Fig. S1) according to the reported method but at an elevated temperature (150 °C) [26]. The as-prepared GQDs had a narrow size distribution largely in the range of 3–5 nm (3.9 ± 0.5 nm, $n=70$) as confirmed by transmission electron microscopy (TEM) images (Fig. 1a, b). The atomic force microscopy (AFM) image (Fig. 1c, d) showed a less than 1-nm height of GQDs (0.6 ± 0.2 nm, $n=100$), indicating that the obtained GQDs primarily consisted of 1–2 graphene layers. Raman spectrum (Fig. S2a) showed an in-plane vibration of sp^2 carbon atom induced G band at 1601 cm^{-1} and a characteristic disorder induced D band at 1350 cm^{-1} [26]. The relatively high intensity of D band and the missing of 2D band indicated the presence of defects in the graphene structure [27,28]. As confirmed by Fourier transform infrared (FTIR) spectra (Fig. S2b) and X-ray photoelectron spectroscopy (XPS) spectra (Fig. S2c, d and e), oxygen-containing functional groups, including carbonyl, carboxyl, hydroxyl and epoxy groups, were introduced to the edge and the basal plane of the nano-sized graphene sheet. XPS spectra showed a graphitic C1s peak at 284.8 eV and O1s peak at 533.0 eV (Fig. S2c) with increased oxygen content after oxidization. High-resolution XPS C1s spectra of carbon fibers and GQDs (Fig. S2d, Se) clearly demonstrated the presence of above mentioned oxygen-containing functional groups on GQDs [26].

The UV–vis absorption spectrum of GQDs had a typical absorption of graphene derivatives in the UV region (200–300 nm) with a peak at 230 nm which was assigned to the π–π^* transition of aromatic sp^2 domains (Fig. 2a). There were two excitation peaks at 265 nm and 351 nm and an emission peak at about 411 nm (Fig. 2b). Unlike reported results [26,29], the emission wavelength of the as-prepared GQDs was only slightly affected by the excitation wavelength (Fig. 2c), implying the ultrafine structure of GQDs which could be attributed to sufficient oxidation at 150 °C. Photoluminescence intensity and maximum emission were pH dependent showing an increased intensity and a blue-shifted emission wavelength with the ascending pH (Fig. 2d). The pH-dependent luminescence supported the mechanism that free zigzag sites on the edge of GQDs with a carbene-like triplet ground state ($\sigma^1\pi^1$) might be the emissive defects [29].

3.2. The quenching effect of transition metal ions on the PL of GQDs

Metal ions can interact with GQDs by chelating with oxygen functional groups on GQDs and the π system of graphene structure of GQDs [30]. In our study, the metal ion was first added to the GQD solution and the change of photoluminescence was detected. EDTA was used as a competitive chelating agent to react with the metal ion to recover quenched photoluminescence.

Interestingly, the above quenching-recovering performance is dramatically diverse and associated with the specific electron configuration of an individual metal ion (Figs. 3 and S3). The metal ions in the non-quenching group are diamagnetic ions with empty or completely filled *d* shell, i.e., a closed shell electron configuration. This stable energy state makes it difficult for electron transfer between GQDs and metal ions, thus no significant effect on the luminescence of GQDs was observed.

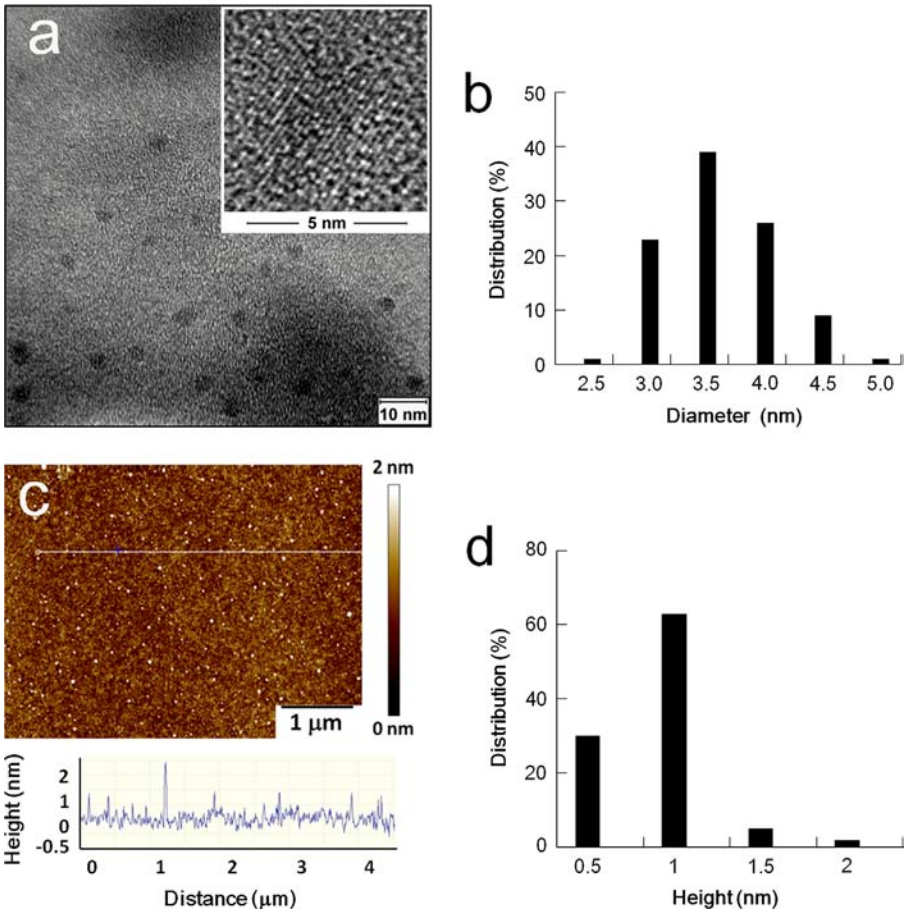

Fig. 1. (a) TEM and HRTEM (inset) images of the GQDs. (b) Diameter distribution of the GQDs. (c) AFM image of the GQDs deposited on the silicon substrate and the height profile along the line as indicated in the image. (d) Height distribution of the GQDs.

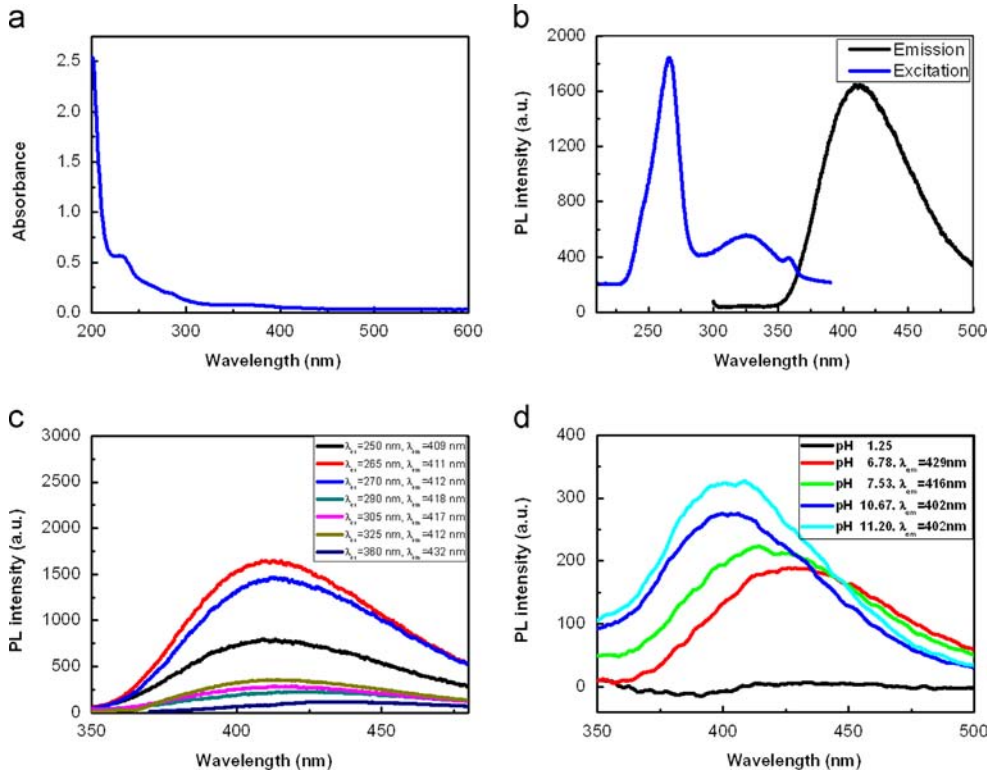

Fig. 2. (a) UV–vis absorption spectrum of GQDs. (b) Excitation and emission spectra of GQDs. Maximum excitation and emission wavelengths were 265 nm and 411 nm, respectively. (c) Emission spectra showing slight dependence on the excitation wavelength. (d) pH dependence of the emission spectra. The excitation wavelength was 265 nm.

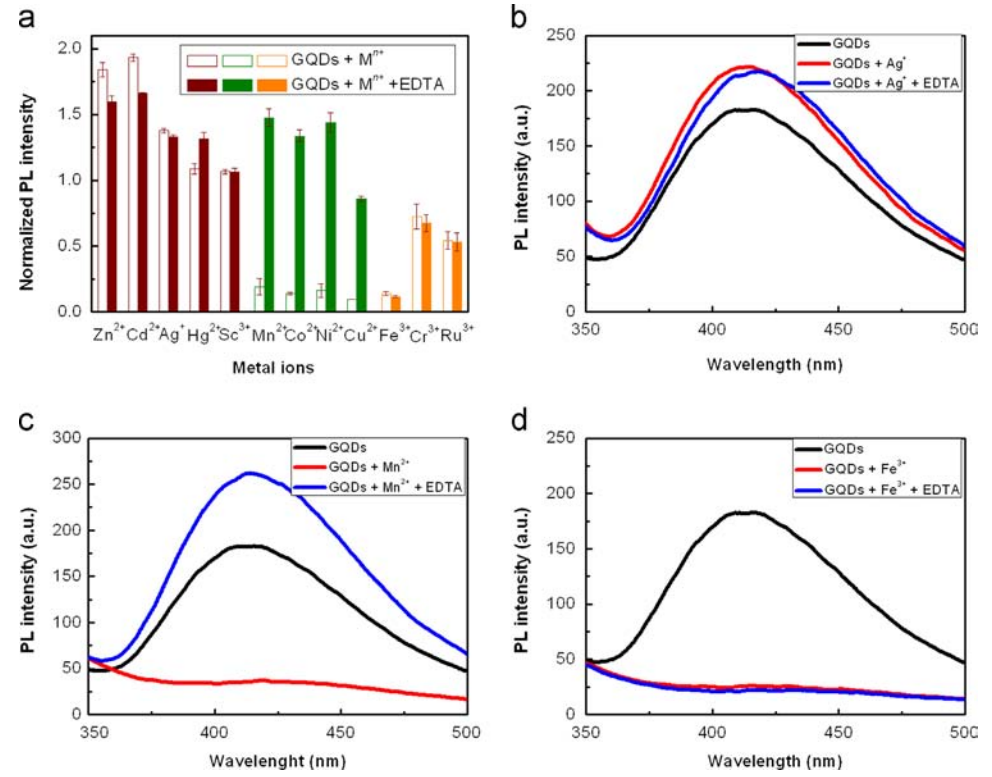

Fig. 3. The categorized quenching-recovering performance of 100 μM metal ions on GQDs (a). The brown, green and orange color denotes the non-quenching, quenching-recovering, and quenching-non-recovering groups, respectively; open and filled columns denote results in the absence and presence of EDTA, respectively. Photoluminescence intensity of GQDs at 411 nm with 265 nm excitation was used for normalization. Representative PL spectra with the addition of metal ions and EDTA in the non-quenching (b), quenching recovering (c) and quenching-non-recovering (d) groups. (For interpretation of the references to color in this figure legend, the reader is referred to the web version of this article.)

For metal ions in the quenching-recovering group, there are partly filled *d* orbits to readily accept electrons from GQDs. It has been reported that carbon nanomaterials with delocalized π-electron systems often serve as the electron donor in the reaction with electron-withdrawing agents [31], e.g. transition metal ions with partly filled *d* orbits. In this occasion, photo-induced electron transfer from GQDs to metal ions can cause perturbation of electronic states of GQDs as well as non-radiative transitions, leading to quenching of the photoluminescence of GQDs. Introducing a competitive chelator, e.g. EDTA, could weaken the interaction between GQDs and metal ions, resulting in recovery of the photoluminescence by releasing GQDs which could then return to their initial electronic states.

For the quenching-non-recovering group, seemingly EDTA was not able to recover the photoluminescence of GQDs, which might be attributed to several reasons. First, Fe^{3+},Cr^{3+} and Ru^{3+} can intensively chelate with the –OH group on the surface of GQDs, considering the low K_{sp} of their metal hydroxides (4×10^{-38} for $Fe(OH)_3$, 6.3×10^{-31} for $Cr(OH)_3$ and 1×10^{-36} for $Ru(OH)_3$). Consequently, strong M–OH interaction resulted in GQD aggregation with addition of Fe^{3+}, Cr^{3+} or Ru^{3+}, making it difficult for EDTA to release GQDs from metal binding. Second, all the three metal ions exhibited absorption in the excitation and emission regions of GQDs (Fig. 4a), while most other metal ions showed minor absorption (Fig. 4b). Therefore, the inner filter effect of Fe^{3+}, Cr^{3+} and Ru^{3+} can be another reason for the inability of photoluminescence recovery. However, we noticed that the presence of Cu^{2+}, which also intensively absorbed light at 265 nm, did not have an effect on the recovery of photoluminescence, indicating that absorption at the emission wavelength is essential for the inability of photoluminescence recovery. Additionally, introducing Fe^{3+} in the GQD solution caused layer aggregation of GQDs as indicated by AFM image (Fig. S4), and a distinctively decreased C=O band was observed for Fe-GQD system in high-resolution XPS C1s spectra (Fig. S5a) compared with Cr-GQD and Ni-GQD systems (Fig. S5b, c). Therefore, we hypothesize that the chelation of Fe^{3+} with delocalized π electrons [30,32] and C=O groups [33] of GQDs, which resulted in aggregation of the graphene sheets, was probably the third reason for the inability of photoluminescence recovery. In this case, steric hindrance made it difficult for EDTA to get access to Fe^{3+} located between the aggregated graphene sheets, hence photoluminescence was not recovered.

3.3. Detection of nickel ion

The above observations about optical property changes indicate the potential of GQDs as an optical platform for metal ion sensing based on a quenching-recovering strategy. To demonstrate the proof-of-concept, a simple, rapid and selective detection method was developed by taking Ni^{2+} as an example. Dimethylglyoxime (DMG), a chelator commonly used in spectrophotometric methods to specifically detect Ni^{2+} [34], was used to replace EDTA as a recovery agent to achieve the selective detection of Ni^{2+}. With DMG at an optimized concentration (Fig. S6), the linear range for Ni^{2+} was up to 90 μM in both standard solution and tap water (Fig. 5 and Fig. S7). The detection limit was 4.1 μM (3σ of the reagent blank signal) in standard solution, which was comparable with most optical methods without sample enrichment or signal amplification (Table S1). Other metal ions in the quenching-recovering group showed no recovery of luminescence over the entire concentration range studied (Fig. S8). This strategy in principle can be applied to the detection of other metal ions by simply selecting specific chelators for metal ions of interest, thus presenting a promising approach for rapid, economical and even multichannel detection of complex metal ion mixtures.

4. Conclusion

In summary, this is the first systematic investigation about the quenching and recovering performance of transition metal ions on the photoluminescence of GQDs, which is one member in the carbon material family. The quenching effect of transition metal ions on the photoluminescence of GQDs was mainly associated with electron configuration of the individual metal ion. This study helps with more profound understanding of the interaction mechanism between GQDs with analytes and better extending the application of GQDs in the optical sensing field. No further functionalization for these structurally defined GQDs was

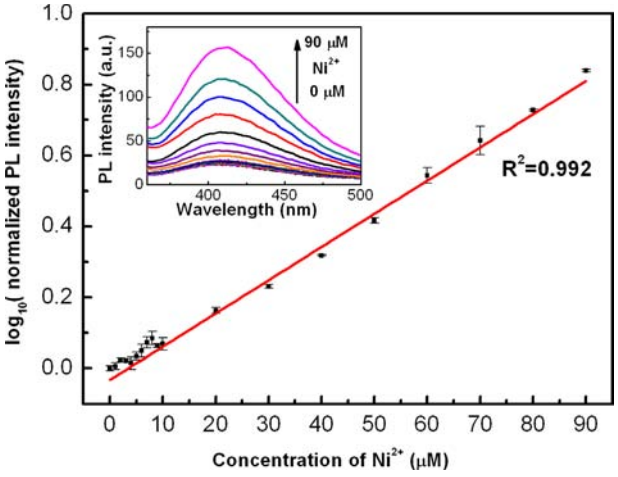

Fig. 5. The photoluminescence intensity recovery at 411 nm (λ_{ex}=265 nm) as a function of Ni^{2+} concentration. Inset shows the associated PL spectral changes.

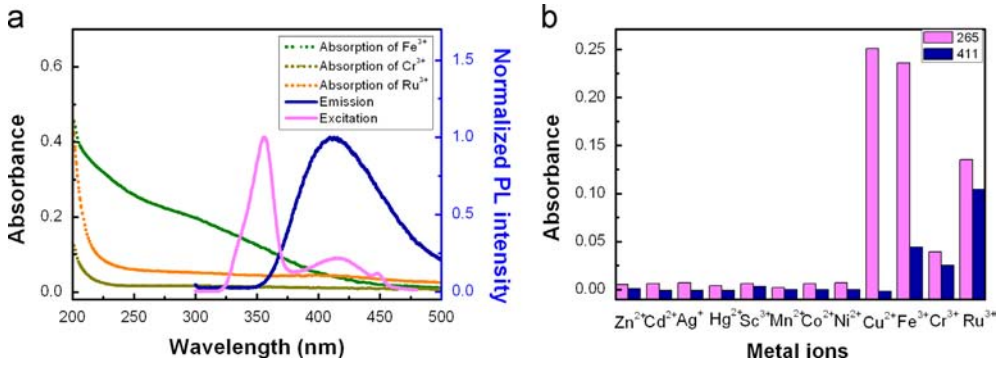

Fig. 4. (a) The overlay of absorption spectra of Fe^{3+}, Cr^{3+} and Ru^{3+} with excitation and emission spectra of GQDs, showing the inner filter effect. (b) Absorption of metal ions at the excitation (265 nm) and emission (411 nm) wavelengths of GQDs.

required, and by using the specific chelating reagent, metal ions in the quenching-recovering group could be detected, as the example of Ni^{2+}, indicative of the simplicity and versatility of this GQD based optical sensing method, and the great promise in metal ion sensing applications.

Acknowledgments

This work was supported by the National Natural Science Foundation of China (Nos. 21035005, 20975004, and 21275011).

Appendix A. Supplementary material

Supplementary data associated with this article can be found in the online version at http://dx.doi.org/10.1016/j.talanta.2013.08.055.

References

[1] X.M. Sun, Z. Liu, K. Welsher, J.T. Robinson, A. Goodwin, S. Zaric, H.J. Dai, Nano Res. 1 (2008) 203–212.
[2] O. Voznyy, A.D. Guclu, P. Potasz, P. Hawrylak, Phys. Rev. B 83 (2011) 165417.
[3] B. Wunsch, T. Stauber, F. Guinea, Phys. Rev. B 77 (2008) 035316.
[4] Z.Z. Zhang, K. Chang, Phys. Rev. B 77 (2008) 235411.
[5] L.A. Ponomarenko, F. Schedin, M.I. Katsnelson, R. Yang, E.W. Hill, K.S. Novoselov, A.K. Geim, Science 320 (2008) 356–358.
[6] S.N. Baker, G.A. Baker, Angew. Chem. Int. Ed. 49 (2010) 6726–6744.
[7] J.H. Shen, Y.H. Zhu, X.L. Yang, C.Z. Li, Chem. Commun. 48 (2012) 3686–3699.
[8] S.J. Zhu, S.J. Tang, J.H. Zhang, B. Yang, Chem. Commun. 48 (2012) 4527–4539.
[9] K.P. Loh, Q.L. Bao, G. Eda, M. Chhowalla, Nat. Chem. 2 (2010) 1015–1024.
[10] Y. Li, Y. Zhao, H.H. Cheng, Y. Hu, G.Q. Shi, L.M. Dai, L.T. Qu, J. Am. Chem. Soc. 134 (2012) 15–18.
[11] Y. Li, Y. Hu, Y. Zhao, G.Q. Shi, L.E. Deng, Y.B. Hou, L.T. Qu, Adv. Mater. 23 (2011) 776–780.
[12] V. Gupta, N. Chaudhary, R. Srivastava, G.D. Sharma, R. Bhardwaj, S. Chand, J. Am. Chem. Soc. 133 (2011) 9960–9963.
[13] X. Yan, X. Cui, B.S. Li, L.S. Li, Nano Lett. 10 (2010) 1869–1873.
[14] Y.Q. Dong, R.X. Wang, G.L. Li, C.Q. Chen, Y.W. Chi, G.N. Chen, Anal. Chem. 84 (2012) 6220–6224.
[15] A.W. Zhu, Q. Qu, X.L. Shao, B. Kong, Y. Tian, Angew. Chem. Int. Ed. 51 (2012) 7185–7189.
[16] H.X. Zhao, L.Q. Liu, Z.D. Liu, Y. Wang, X.J. Zhaoa, C.Z. Huang, Chem. Commun. 47 (2011) 2604–2606.
[17] Q. Qu, A.W. Zhu, X.L. Shao, G.Y. Shi, Y. Tian, Chem. Commun. 48 (2012) 5473–5475.
[18] J.C.G.E. da Silva, H.M.R. Goncalves, TrAC Trends Anal. Chem. 30 (2011) 1327–1336.
[19] H.M.R. Goncalves, A.J. Duarte, J.C.G.E. da Silva, Biosens. Bioelectron. 26 (2010) 1302–1306.
[20] L. Cao, X. Wang, M.J. Meziani, F.S. Lu, H.F. Wang, P.J.G. Luo, Y. Lin, B.A. Harruff, L.M. Veca, D. Murray, S.Y. Xie, Y.P. Sun, J. Am. Chem. Soc. 129 (2007) 11318–11319.
[21] S.T. Yang, L. Cao, P.G.J. Luo, F.S. Lu, X. Wang, H.F. Wang, M.J. Meziani, Y.F. Liu, G. Qi, Y.P. Sun, J. Am. Chem. Soc. 131 (2009) 11308–11309.
[22] J.L. Chen, X.P. Yan, K. Meng, S.F. Wang, Anal. Chem. 83 (2011) 8787–8793.
[23] Y. Dong, G. Li, N. Zhou, R. Wang, Y. Chi, G. Chen, Anal. Chem. 84 (2012) 8378–8382.
[24] D. Wang, L. Wang, X.Y. Dong, Z. Shi, J. Jin, Carbon 50 (2012) 2147–2154.
[25] A. Kundu, R.K. Layek, A.K. Nandi, J. Mater. Chem. 22 (2012) 8139–8144.
[26] J. Peng, W. Gao, B.K. Gupta, Z. Liu, R. Romero-Aburto, L.H. Ge, L. Song, L.B. Alemany, X.B. Zhan, G.H. Gao, S.A. Vithayathil, B.A. Kaipparettu, A. A. Marti, T. Hayashi, J.J. Zhu, P.M. Ajayan, Nano Lett. 12 (2012) 844–849.
[27] A.C. Ferrari, J.C. Meyer, V. Scardaci, C. Casiraghi, M. Lazzeri, F. Mauri, S. Piscanec, D. Jiang, K.S. Novoselov, S. Roth, A.K. Geim, Phys. Rev. Lett. 97 (2006) 187401.
[28] A.C. Ferrari, J. Robertson, Phys. Rev. B 61 (2000) 14095–14107.
[29] D.Y. Pan, J.C. Zhang, Z. Li, M.H. Wu, Adv. Mater. 22 (2010) 734–738.
[30] S. Park, K.S. Lee, G. Bozoklu, W. Cai, S.T. Nguyen, R.S. Ruoff, ACS Nano 2 (2008) 572–578.
[31] P.W. Barone, S. Baik, D.A. Heller, M.S. Strano, Nat. Mater. 4 (2005) 86. (U16).
[32] S.A. Miller, J.A. Tebboth, J.F. Tremaine, J. Chem. Soc. (1952) 632–635.
[33] C.W. Bauschlicher, P.S. Bagus, J. Chem. Phys. 81 (1984) 5889–5898.
[34] A.M. Mitchell, M.G. Mellon, Ind. Eng. Chem. Anal. Ed. 17 (1945) 380–382.